JOURNAL

OF THE AMERICAN CHEMICAL SOCIETY

VOLUME 108, NUMBER 3 FEBRUARY 5, 1986

Mechanism for the Oscillatory Bromate–Iodide Reaction[1]

Ofra Citri and Irving R. Epstein*

Contribution from the Department of Chemistry, Brandeis University, Waltham, Massachusetts 02254. *Received August 12, 1985*

Abstract: A mechanism is proposed for the reaction between bromate and iodide ions in acidic solution. The mechanism consists of 13 elementary steps and involves the interhalogen compound IBr but does not contain any radical species. Extensive numerical simulations show that the mechanism gives good agreement with the observed "clock" behavior in batch and with the bistability and oscillations observed in a CSTR. The present system appears to be the first in which bistability between a stationary and an oscillatory state has been successfully described by a mechanism consisting of elementary steps.

Perhaps the most convincing proof of the progress chemists have made in understanding chemical oscillation is to be found in the excellent agreement obtained between predictions derived from the mechanisms proposed for oscillating reactions and the complex experimental behavior which they exhibit. Since Field, Körös, and Noyes' (FKN) classic breakthrough in modeling the Belousov–Zhabotinsky (BZ) reaction,[2] successful mechanisms have been developed for the Bray–Liebhafsky,[3] Briggs-Rauscher,[4,5] and, most recently, systematically designed chlorite–iodide[6] oscillators. Even the temperature dependence of oscillations in the minimal bromate oscillator has been explained by using a simplified version of the FKN mechanism.[7]

While efforts to model bistability and oscillations have been remarkably fruitful, the mechanistic study of more complex dynamical behavior such as chaos, birhythmicity, and bistability between steady and oscillatory states is in a less-developed state. Calculations on certain forms of chaos in the BZ system[8] have appeared, and birhythmicity has been predicted from calculations on a coupled enzyme model,[9] but so far no full mechanistic description of a chemical system showing these dynamic phenomena has been achieved. The BrO_3^-–ClO_2^-–I^- coupled system, which shows both chaos[10] and birhythmicity,[11] is a prime candidate for efforts in this direction. Finding mechanisms for each of the component systems, ClO_2^-–I^- and BrO_3^-–I^-, which show rich dynamical behavior by themselves, is a promising way to approach a mechanistic model of the more complex coupled system. Since a mechanism for the ClO_2^-–I^- system has already been proposed,[6] the next logical step is to develop a mechanism for the BrO_3^-–I^- system.[12]

We present here a mechanistic study of the BrO_3^-–I^- reaction. In addition to simulating the bistability and oscillations observed in a flow reactor (CSTR), our mechanism gives excellent agreement with the clock behavior exhibited by the reaction in a closed system and with the bistability between stable stationary and oscillatory states found with certain flow conditions. This last feature has not previously, to our knowledge, been predicted in any other mechanistically based calculation on a chemical oscillator.

Experimental Background

Closed System. In an acidic medium and in an excess of bromate, the reaction between bromate and iodide proceeds in two stages:

$$6I^- + 6H^+ + BrO_3^- \rightarrow 3I_2 + 3H_2O + Br^- \quad (1)$$

$$I_2 + 2BrO_3^- \rightarrow Br_2 + 2IO_3^- \quad (2)$$

The first stage shows quite simple kinetics and obeys the rate law

$$\frac{-d[BrO_3^-]}{dt} = k_1[H^+]^2[BrO_3^-][I^-] \quad (3)$$

with k_1 = 40–50 M^{-3} s^{-1}.[13]

Reaction 2 was studied by King and Lister,[14] who found it to be considerably more complex, proceeding in four stages: an induction period, a period of simultaneous disappearance of I_2 and production of IBr, a period of disappearance of IBr, and, finally, a period of the slow appearance of Br_2.

Recently, Simoyi[13] has reinvestigated reactions 1 and 2. He finds that the oxidation of I_2 by BrO_3^- does not begin until reaction 1 is essentially complete, i.e., until $[I_2]$ has reached its maximum value of $^1/_2$ $[I^-]_0$. This result is in agreement with the induction time observed by King and Lister in reaction 2, which they equate to the time required for removal of I^- from the system. Once I_2 reaches its maximum concentration, it is consumed rapidly in a typical "clock reaction". Figure 1a shows traces of the I_2 absorbance during the two stages of the reaction at two slightly different acid concentrations.[13]

(1) Part 33 in the series Systematic Design of Chemical Oscillators. Part 32: Nagypal, I.; Epstein, I. R.; Kustin, K. *Int. J. Chem. Kinet.*, in press.
(2) Field, R. J.; Körös, E.; Noyes, R. M. *J. Am. Chem. Soc.* **1972**, *94*, 8649.
(3) Sharma, K. R.; Noyes, R. M. *J. Am. Chem. Soc.* **1976**, *98*, 4345.
(4) Noyes, R. M.; Furrow, S. D. *J. Am. Chem. Soc.* **1982**, *104*, 45.
(5) De Kepper, P.; Epstein, I. R. *J. Am. Chem. Soc.* **1982**, *104*, 49.
(6) Epstein, I. R.; Kustin, K. *J. Phys. Chem.* **1985**, *89*, 2275.
(7) Kumpinsky, E.; Epstein, I. R. *J. Phys. Chem.* **1985**, *89*, 688.
(8) (a) Turner, J. S. In "Self Organization in Dissipative Structures"; Schieve, W. D.; Allen, P., Eds.; University of Texas Press: Austin, 1982; p 41. (b) Richetti, P.; Arneodo, A., unpublished results.
(9) Decroly, O.; Goldbeter, A. *Proc. Natl. Acad. Sci. U.S.A.* **1982**, *79*, 6917.
(10) Masełko, J.; Alamgir, M.; Epstein, I. R. *Physica D*, in press.
(11) Alamgir, M.; Epstein, I. R. *J. Am. Chem. Soc.* **1983**, *105*, 2500.
(12) Alamgir, M.; De Kepper, P.; Orbán, M.; Epstein, I. R. *J. Am. Chem. Soc.* **1983**, *105*, 2641.
(13) Simoyi, R. *J. Phys. Chem.*, in press.
(14) King, D. E. C.; Lister, M. W. *Can. J. Chem.* **1968**, *46*, 279.

0002-7863/86/1508-0357$01.50/0

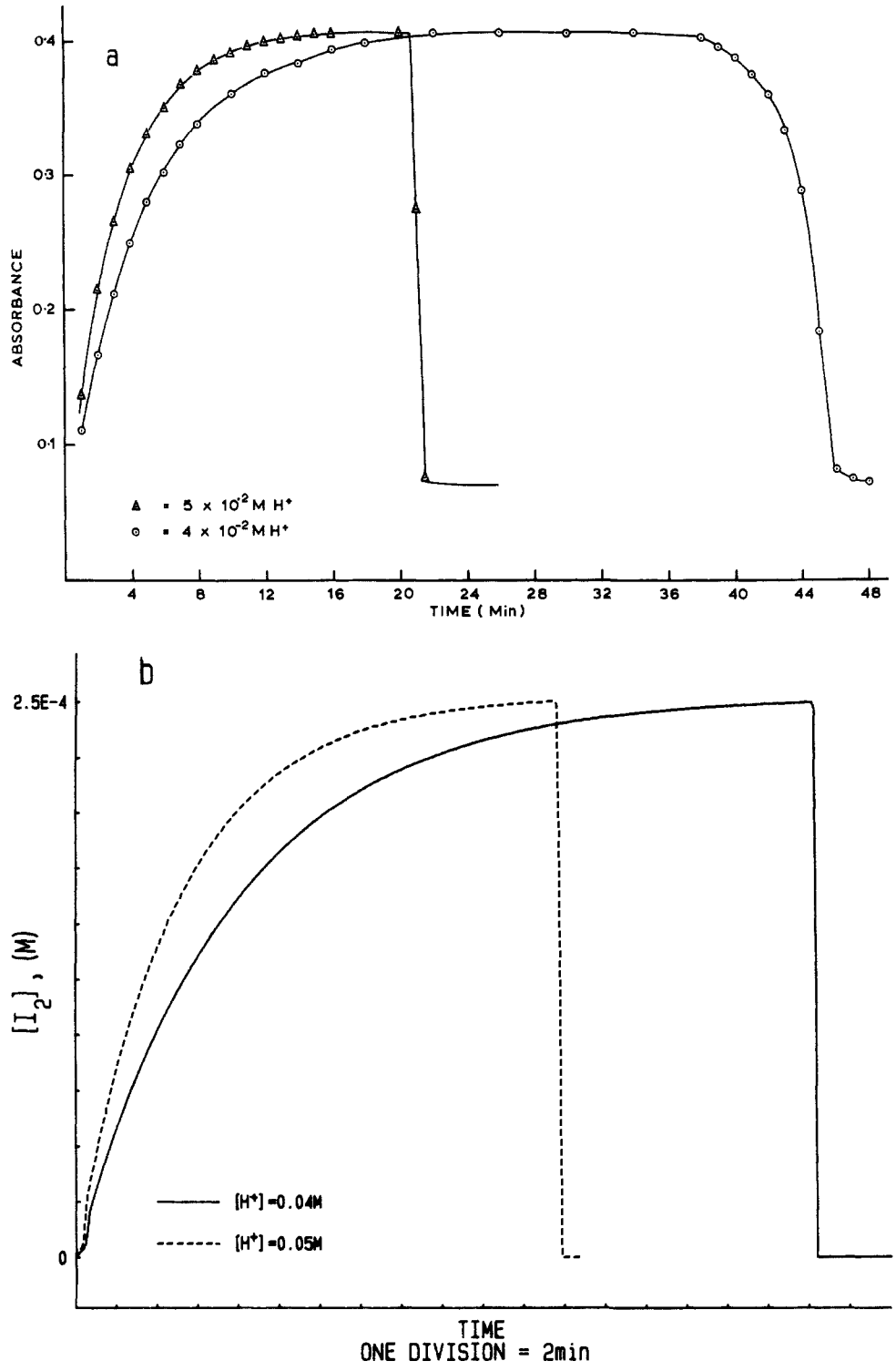

Figure 1. Iodine concentration as a function of time in the batch reaction at two acid concentrations: (a) experimental absorbance at 460 nm;[13] (b) calculated $[I_2]$. Initial conditions: $[BrO_3^-] = 5 \times 10^{-3}$ M, $[I^-] = 5 \times 10^{-4}$ M.

Open System. Alamgir et al.[12] studied the bromate–iodide reaction in a CSTR, obtaining the phase diagram shown in Figure 2a. We shall discuss their results as well as others we have obtained by using a similar apparatus but at somewhat different input concentrations and flow rates. Detailed descriptions of the experimental setup as well as of the methods used to obtain the hysteresis curves and phase diagrams are given by De Kepper et al.[15] and by Orbán and Epstein.[16]

In a flow reactor, the BrO_3^-–I^- system shows bistability over a range of nearly 5 orders of magnitude in the iodide input concentration $[I^-]_0$. At sufficiently high $[I^-]_0$ and $[BrO_3^-]_0$, sustained oscillations are observed. At intermediate $[I^-]_0$, the system exhibits a Hopf bifurcation.[17] The oscillatory state can be reached from only one of the two steady states, giving rise to hysteresis and a region of bistability between a stationary and an oscillatory state as shown in Figure 3.

The two steady states may be distinguished visually. The flow branch SSI is brown, while the thermodynamic branch SSII is yellow. SSI has a lower redox potential and an absorbance maximum at 460 nm (I_2), while SSII has a higher redox potential and shows maximum absorbance at 390–400 nm. We attribute this latter peak to Br_2 and/or IBr which have similar spectra in aqueous solution.[14,18,19]

(15) De Kepper, P.; Epstein, I. R.; Kustin, K. *J. Am. Chem. Soc.* **1981**, *103*, 6121.
(16) Orbán, M.; Epstein, I. R. *J. Am. Chem. Soc.* **1985**, *107*, 2302.
(17) Marsden, J.; McCracken, M. "The Hopf Bifurcation and Its Applications"; Springer-Verlag: New York, 1976.
(18) Gillam, A. E. *Trans. Faraday Soc.* **1933**, *29*, 1132.

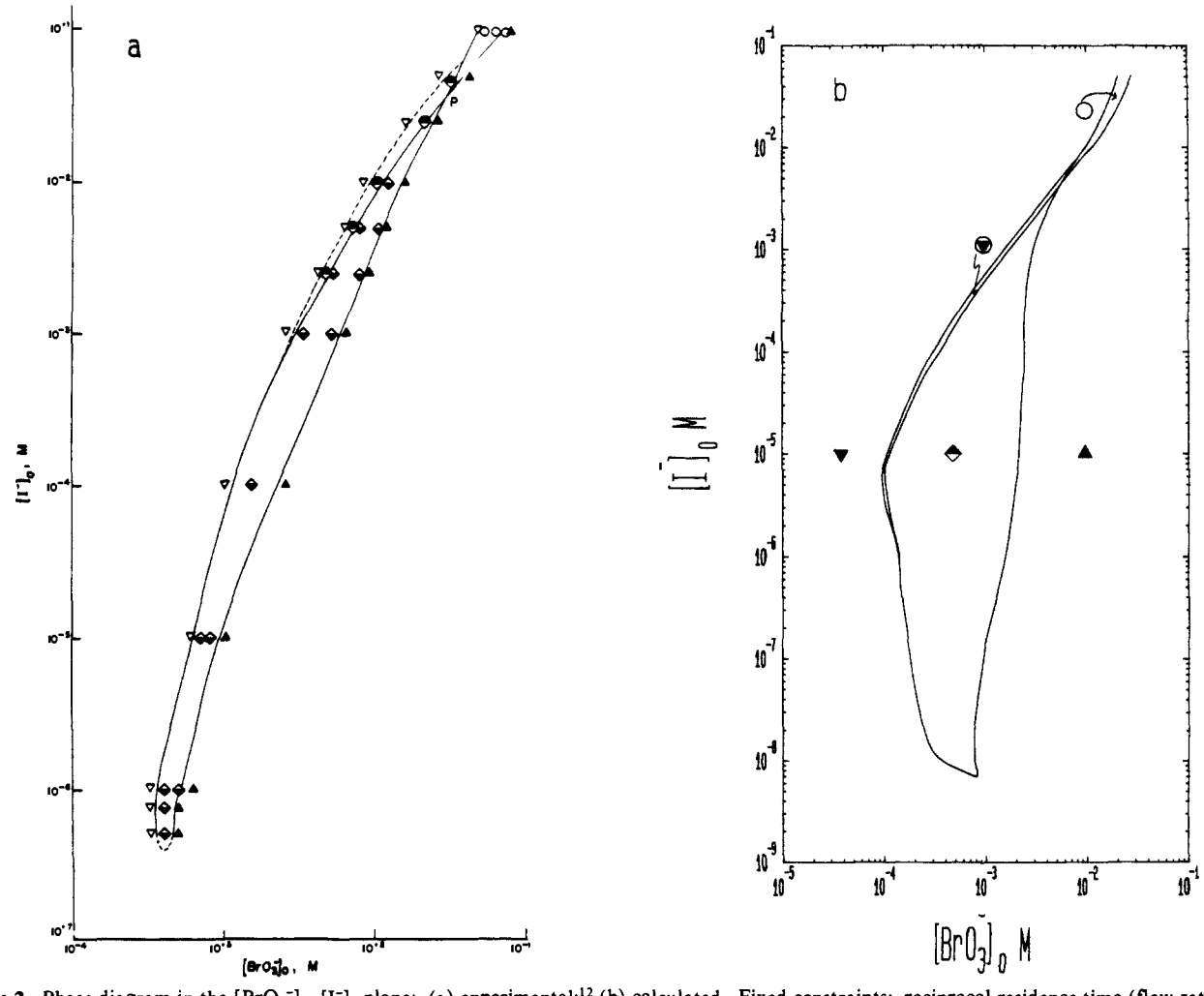

Figure 2. Phase diagram in the $[BrO_3^-]_0$–$[I^-]_0$ plane: (a) experimental;[12] (b) calculated. Fixed constraints: reciprocal residence time (flow rate) $k_0 = 1.2 \times 10^{-2}$ s^{-1}, $[H^+]_0 = 1.5$ M. Symbols: (▽,▼) SSI; (▲) SSII; (◈) bistability between SSI and SIII; (○) oscillation; (◉) bistability between oscillatory state and SSI.

Evidence that at least a major portion of the absorbance in SSII results from IBr has been obtained as follows. When the system was in SSII, samples were removed from the CSTR and extracted with CCl_4, a solvent in which IBr and Br_2 have significantly different absorbances. The UV–vis spectrum obtained immediately after extraction matched closely that of IBr in CCl_4.[18] However, samples which were examined at longer times after removal from the reactor showed spectra more closely resembling that of Br_2 in CCl_4.

The oscillations, typical traces of which are given in Figure 4, are seen as the appearance and disappearance of a brown color on a yellow background. Bromide and iodide selective electrodes show parallel traces. The simulations show $[I^-]$ to be negligible. Therefore, we have assumed that the ion-selective electrodes respond primarily to Br^- and have calibrated them accordingly. The $[Br^-]$ levels measured in the two steady states are almost identical, though during the transition from SSI to SSII the bromide electrode shows a sharp decrease in $[Br^-]$. Immediately after this dip, the bromide level increases to nearly its original value.

Constructing the Mechanism

Choice of Reactions. On the basis of King and Lister's studies and our own qualitative observations, we postulate four major overall processes in the reaction.

$$BrO_3^- + 6I^- + 6H^+ \rightarrow 3I_2 + Br^- + 3H_2O \qquad (O1)$$

$$I_2 + BrO_3^- \rightarrow IBr + IO_3^- \qquad (O2)$$

$$IBr + BrO_3^- \rightarrow Br_2 + IO_3^- \qquad (O3)$$

$$BrO_3^- + 5Br^- + 6H^+ \rightarrow 3Br_2 + H_2O \qquad (O4)$$

Process O1 is the first stage of the batch bromate–iodide reaction and dominates SSI under flow conditions. As the concentration of iodide decreases, either by consumption in process O1 or in the CSTR by decreasing the inflow of iodide, processes O2 and O3 begin. Iodide is now consumed, while IBr and Br_2 are generated, giving rise under flow conditions to the yellow, low-I_2, steady state. Process O4 is the slowest of the group and is significant only toward the end of the batch reaction or at very low flow rates in the CSTR. Thus, since Br^- is neither produced nor consumed in processes O2 and O3,[20] no significant difference is to be expected between the bromide levels in the two steady states, and none is observed experimentally.

Next, it is necessary to dissect the overall processes (O1)–(O4) into elementary steps. Where possible, we have proceeded by analogy with the known mechanism for other oxyhalogen oscillators, particularly the minimal bromate[21] and chlorite–iodide[6] systems. Of course, the present system requires the addition of reactions specifically involving the chemistry of IBr. Here we have adopted King and Lister's suggestion[14] that the first step in the BrO_3^-–I_2 reaction is

$$I_2 + HOBr \rightarrow IBr + HOI \qquad (E6)$$

Our proposed mechanism is given in Table I. In addition to IBr, the scheme involves the most stable of the known closed-shell oxybromine and oxyiodine species.

(19) Cremer, H. W.; Duncan, O. R. *J. Chem. Soc.* **1932**, 2031.

(20) Though it may participate in a kinetically, but nonstoichiometrically, significant fashion in these processes.

(21) Noyes, R. M.; Field, R. J.; Thompson, R. C. *J. Am. Chem. Soc.* **1971**, *93*, 7315.

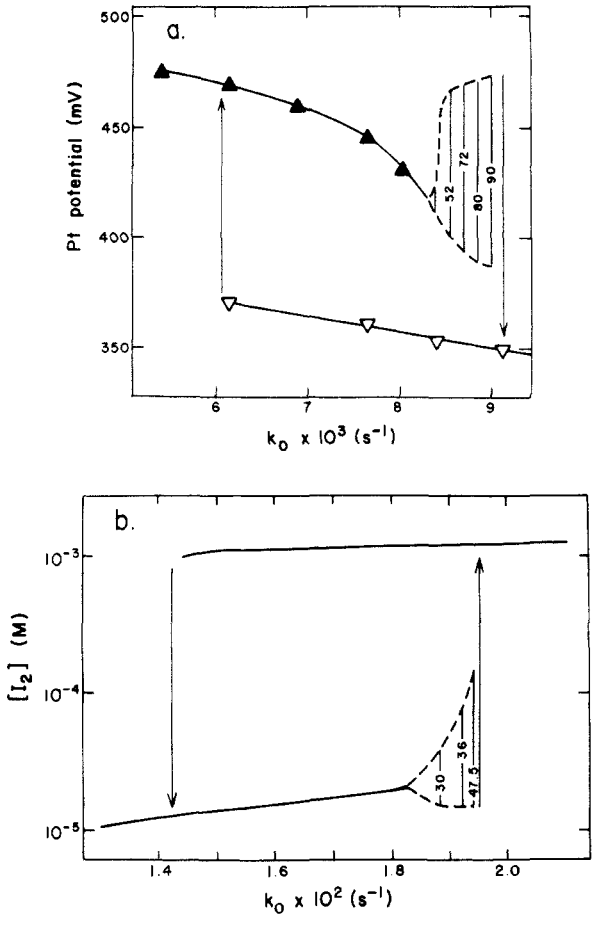

Figure 3. Bistability and hysteresis as a function of flow rate between stationary and oscillatory states. Arrows indicate points of transition: (a) experimental redox potential (vs. $Hg|Hg_2SO_4|K_2SO_4$ reference electrode); (b) calculated $[I_2]$. Fixed constraints: $[BrO_3^-]_0 = 5 \times 10^{-3}$ M, $[I^-]_0 = 2.5 \times 10^{-3}$ M, $[H^+]_0 = 1.5$ M. Note that high Pt potential corresponds to low $[I_2]$.

Table I. Elementary Steps in the Mechanism

no.	reaction	k_f[a]	k_r[a]
(E1)	$2H^+ + BrO_3^- + I^- \rightarrow HBrO_2 + HOI$	45	
(E2)	$HBrO_2 + HOI \rightarrow HIO_2 + HOBr$	1×10^9	
(E3)	$I^- + HOI + H^+ = I_2 + H_2O$	3.1×10^{12}	2.2
(E4)	$BrO_3^- + HOI + H^+ \rightarrow HBrO_2 + HIO_2$	8×10^2	
(E5)	$BrO_3^- + HIO_2 \rightarrow IO_3^- + HBrO_2$	1.6×10^4	
(E6)	$HOBr + I_2 = HOI + IBr$	8×10^7	1×10^2
(E7)	$IBr + H_2O = HOI + Br^- + H^+$	3×10^1	1×10^8
(E8)	$HBrO_2 + Br^- + H^+ \rightarrow 2HOBr$	2×10^6	
(E9)	$HOBr + Br^- + H^+ = Br_2 + H_2O$	8×10^9	1.1×10^2
(E10)	$BrO_3^- + Br^- + 2H^+ = HBrO_2 + HOBr$	2.1	1×10^4
(E11)	$Br^- + HIO_2 + H^+ = HOI + HOBr$	6×10^5	2×10^8
(E12)	$HIO_2 + HOBr \rightarrow IO_3^- + Br^- + 2H^+$	2.25×10^8	
(E13)	$BrO_3^- + IBr + H_2O \rightarrow IO_3^- + Br^- + HOBr + H^+$	8×10^{-1}	

[a] All concentrations in M; times in s.

The reactions in Table I can be combined in appropriate sets to generate the stoichiometries of each of the overall processes (O1)–(O4). At earlier stages, other reactions such as the disproportionation of HIO_2 and $HBrO_2$ and the reaction between them were included in our scheme. Since these steps proceeded at negligible rates with rate constants up to 10^7 M^{-1} s^{-1} for the first two reactions and 10^6 M^{-1} s^{-1} for the third,[22] they were omitted from the final version of the mechanism.

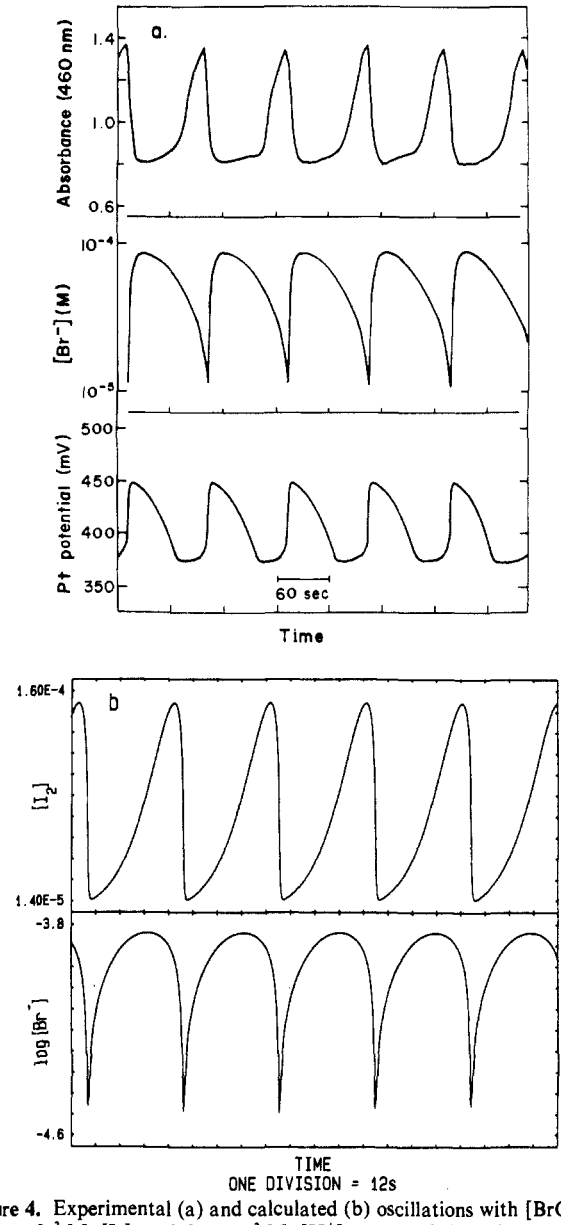

Figure 4. Experimental (a) and calculated (b) oscillations with $[BrO_3^-]_0 = 5 \times 10^{-3}$ M, $[I^-]_0 = 2.5 \times 10^{-3}$ M, $[H^+]_0 = 1.5$ M, $k_0 = 9 \times 10^{-3}$ s^{-1} (a), 1.94×10^{-2} s^{-1} (b).

With the exception of step E13, all the proposed elementary reactions involve the transfer of a single oxygen atom. Reaction E13 is more complex and probably is not a true elementary step. It might proceed by a sequence of kinetically equivalent simpler reactions such as

$$H^+ + BrO_3^- + IBr = IBrO_2 + HOBr \text{ (rapid equilibrium)}$$

$$IBrO_2 + H_2O \rightarrow IO_3^- + Br^- + 2H^+ \text{ (slow)}$$

In fact, reaction E13 is not essential for the qualitative behavior of the mechanism,[23] though it does improve slightly the quantitative agreement with experiment. Adjustment of the other rate constants might allow its complete elimination. In order to simplify the model, no distinction has been made between protonated and unprotonated species. No trihalide ions have been considered, though at the bromide concentrations found such species as Br_3^-, IBr_2^-, and I_2Br^- might well be present in nonnegligible amounts.

Rate Constants. Of the initial set of 26 forward and reverse rate constants for reactions E1–E13, only seven, k_1, k_3, k_{-3}, k_8, k_9, k_{-9}, and k_{10}, are known experimentally with any degree of

(22) Higher values of the HIO_2–$HBrO_2$ rate constant actually worsen the agreement between simulation and experiment.

(23) (E13) is stoichiometrically equivalent to (E2) + (E7) + (E10) + (E12) or to (E4) + (E7) + (E8) + (E12).

accuracy. From thermodynamic data,[21] the equilibrium constants for reactions E6 and E7 may be calculated to be approximately 10^6 and 10^{-7}, respectively, reducing the number of "free" parameters by two. Using reasonable estimates for the free energies of formation of $HBrO_2$[2] and HIO_2,[3,24] we find that the equilibria in reactions E1, E2, E5, E8, E12, and E13 all lie far to the right. We thus treat these reactions as irreversible and drop the corresponding reverse rate constants. While the equilibrium constant for reaction E4 should be significantly less than unity, including values of k_{-4} as high as 10^6 M^{-1} s^{-1} had no effect on the calculated behavior of the system. We thus set k_{-4} to zero. The remaining rate constants were chosen initially by analogy with related oxyhalogen reactions as detailed below. Final values were then established by extensive comparison of computed and experimental data.

Reaction E1. The value of k_1 was taken from the work of Simoyi,[13] though that work was performed under somewhat different conditions. Other literature values[25] range from 40 to 50 M^{-3} s^{-1}. The value of this rate constant has no effect on the calculated CSTR results.

Reaction E2. This should be a rapid oxygen transfer. The corresponding reaction between $HClO_2$ and HOI has a rate constant[26] of 6×10^7 M^{-1} s^{-1}.

Reaction E3. These values are taken from the stopped-flow study of Eigen and Kustin.[27]

Reaction E4. The analogous conproportionation rates of $HBrO_2$[28] and of HIO_2[4] are generally considered to be quite slow, but no direct experimental measurements could be found. The value of k_4 affects significantly the parameter (k_0, input concentration) values for the transition from SSI to SSII.

Reaction E5, E6, and E7. Lacking relevant data, we chose k_5, k_6, and k_7 by comparison of calculated and experimental phase diagrams. The value of k_6 is the major determinant of $[I_2]$ in SSII, with higher k_6 giving lower $[I_2]$. The results do not depend upon k_7 but only upon the equilibrium constant k_7/k_{-7}.

Reaction E8. The value chosen for k_8 is from the experimental work of Noszticzius et al.[29] Other studies[2] have used values as high as 1×10^9 M^{-2} s^{-1}.

Reaction E9. These values were measured by Eigen and Kustin.[27]

Reaction E10. The values used are those of Field et al.[2]

Reaction E11. Our value for k_{11} lies between those employed for $HClO_2 + I^-$ and $HIO_2 + I^-$ in the chlorite–iodide study,[6] while k_{-11} is equal to the rate constant used there for the reaction between HOI and HOCl.

Reaction E12. The rate constant found here differs negligibly from that of the HIO_2 + HOCl reaction in ref 6.

Reaction E13. As noted above, this reaction should be slow and might possibly be neglected. The value chosen is the one that gives the best agreement with the data.

Note Added in Proof. At the high acidities employed in these studies, the forward rate constants which appear in Table I for reactions E3 and E9 exceed the diffusion-controlled limit. More careful analysis of ref 27 shows that at high $[H^+]$ the appropriate expressions are $k_3 = 5 \times 10^9/([H^+] + 2 \times 10^{-3})$, $k_9 = 5 \times 10^9/([H^+] + 0.25)$ with all concentrations in M and times in s. Corresponding changes should also be made to allow for the $[H^+]$ dependence of the reverse rates.

Recalculation of the results reported here shows that these corrections produce only very slight changes with the single exception of the $[I^-]$ concentration in SSII, which is increased by about three orders of magnitude, though it still remains negligible (the value given in Table II rises to 3.4×10^{-9} M). The negligible effect of changing the rate constants in this fashion stems from the fact that reactions E3 and E9 are nearly at equilibrium at all times, so that as long as they remain rapid and no change is made in the equilibrium constants there should be no significant effect on the calculated results. We thank Dr. Istvan Nagypal for pointing out the need for this correction, which has apparently been neglected in previous mechanistic studies of other oscillatory reactions.

Calculations and Results

In order to compare the predictions of the mechanism (E1)–(E13) with experiment, one must integrate numerically the derived rate equations augmented in the CSTR case by the flow terms $k_0([X_i]_0 - [X_i])$ where k_0 is the reciprocal of the residence time and $[X_i]_0$ is the input concentration of species X_i corrected for dilution. All the $[X_i]_0$ are zero except for $[BrO_3^-]_0$ and $[I^-]_0$. Although $[H^+]$ was not buffered during the CSTR experiments, the high acidity, 1–1.5 M, suggests that its variation during the course of an experiment may be neglected. Since IO_3^- is an inert product in our mechanism, its concentration need not be calculated. We are left with ten variables of interest: $[BrO_3^-]$, $[I^-]$, $[HBrO_2]$, [HOI], $[HIO_2]$, [HOBr], $[Br^-]$, $[I_2]$, [IBr], and $[Br_2]$.

For each simulation, one must specify the flow rate k_0, the acid concentration $[H^+]$, the input flows $[I^-]_0$ and $[BrO_3^-]_0$, and the initial concentrations of the variable species. In studies designed to search for hysteresis, the final state for one set of parameter values (k_0, $[H^+]$, $[I^-]_0$, and $[BrO_3^-]_0$) served as the initial condition for the next set as a single parameter was varied, simulating the actual experiments. The equations were integrated by using Hindmarsh's version[30] of the Gear algorithm[31] for stiff differential equations. Particularly in the region of the Hopf bifurcation, the parameters must be varied in extremely small steps to avoid inducing a transition from the low I_2 to the high I_2 steady state, thereby missing the oscillating state which is reached if the parameters are changed more slowly. The same behavior is observed experimentally as the pump rate or the input concentrations are varied.

Batch Results. Our mechanism was developed, and most of the simulations were carried out for flow conditions. However, after the major features of the model had been worked out, we became aware of a new study[13] on the batch behavior of the bromate–iodide reaction. We therefore undertook a series of simulations of the kinetics of the BrO_3^-–I^- reaction is a closed system.

The results obtained are shown in Figure 1b. The calculations are in good agreement with the experimental rise in $[I_2]$ and with its rapid consumption at low pH. At slightly higher pH, the model fails to predict the slower disappearance of I_2 observed experimentally. Trial calculations suggest that the time at which $[I_2]$ reaches its maximum depends only upon the rate constant k_1. We have not been able, however, to find a set of rate constants which makes the rate of I_2 disappearance H^+-dependent.

The batch behavior can be understood primarily in terms of reactions E3, E6, and E7. So long as $v_3 > v_6$,[32] any I_2 consumed in (E6) is immediately regenerated by (E3). Adding (E7) gives us a sequence autocatalytic in I_2 if (E6) is rate-determining:

$$2(E3) + (E6) + (E7) = I_2 + 2I^- + HOBr + H^+ \rightarrow 2I_2 + Br^- + H_2O \quad (4)$$

However, when $[I^-]$ becomes sufficiently low, then I_2 is consumed more rapidly by (E6) than it is produced by (E3). Since (E3) is rapid compared with the reactions E2 and E4 which take HOI to HIO_2, essentially all the iodide which is oxidized remains as I_2 until $[I^-]$ drops low enough so that reaction E3 is no longer of major importance. The rapid disappearance of I_2 which then occurs will be discussed below.

(24) *J. Phys. Chem. Ref. Data* **1982**, *11*, Suppl. No. 2.
(25) (a) Barton, A. F. M.; Wright, F. A. *J. Chem. Soc. A* **1968**, 1747. (b) Barton, A. F. M.; Boon-Hiam, L. *J. Chem. Soc. A* **1971**, 3032.
(26) Kern, D. M.; Kim., C. H. *J. Am. Chem. Soc.* **1965**, *87*, 5309.
(27) Eigen, M.; Kustin, K. *J. Am. Chem. Soc.* **1962**, *84*, 1355.
(28) Tyson, J. J. In "Oscillations and Traveling Waves in Chemical Systems"; Field, R. J.; Burger, M., Eds.; Wiley: New York, 1985; p 93.
(29) Noszticzius, Z.; Noszticzius, E.; Schelly, Z. A. *J. Phys. Chem.* **1983**, *87*, 510.
(30) Hindmarsh, A. C. "GEAR: Ordinary Differential Equation Solver"; Lawrence Livermore Laboratory; New York, UCID-30001, Rev. 3.
(31) Gear, C. W. *Commun. ACM* **1971**, *14*, 176.
(32) We use v_i to represent the (net) rate of elementary reaction E_i.

Table II. Calculated Concentrations and Rates in SSI and SSII under Identical (Bistable) Conditions[a]

concn, M	SSI	SSII	rate, M s^{-1}	SSI	SSII
$[BrO_3^-]$	4.5×10^{-3}	3.2×10^{-3}	v_1	1.98×10^{-9}	2.2×10^{-12}
$[I^-]$	8.8×10^{-9}	6.9×10^{-12}	v_2	9.0×10^{-7}	2.4×10^{-5}
$[HBrO_2]$	7.2×10^{-9}	1.0×10^{-8}	v_3	4.0×10^{-5}	4.0×10^{-5}
[HOI]	6.5×10^{-8}	2.3×10^{-6}	v_4	6.7×10^{-7}	8.7×10^{-6}
$[HIO_2]$	2.1×10^{-9}	3.3×10^{-7}	v_5	3.3×10^{-7}	1.7×10^{-5}
[HOBr]	2.4×10^{-10}	3.2×10^{-8}	v_6	2.2×10^{-5}	3.97×10^{-5}
$[Br^-]$	3.4×10^{-4}	9.5×10^{-5}	v_7	1.8×10^{-5}	2.0×10^{-5}
$[I_2]$	1.2×10^{-3}	1.55×10^{-5}	v_8	6.5×10^{-6}	2.9×10^{-6}
[IBr]	1.1×10^{-4}	1.1×10^{-3}	v_9	1.3×10^{-7}	5.3×10^{-6}
$[Br_2]$	9.0×10^{-6}	3.3×10^{-4}	v_{10}	6.4×10^{-6}	1.4×10^{-6}
$[IO_3^-]$	3.2×10^{-5}	1.4×10^{-3}	v_{11}	1.2×10^{-6}	1.4×10^{-5}
			v_{12}	2.5×10^{-10}	2.4×10^{-6}
			v_{13}	6.7×10^{-7}	2.7×10^{-6}

[a] $[I^-]_0 = 2.5 \times 10^{-3}$ M, $[BrO_3^-]_0 = 5 \times 10^{-3}$ M, $[H^+] = 1.5$ M, $k_0 = 1.6 \times 10^{-2}$ s^{-1}.

Flow Results. In Figure 2, we compare the calculated and experimental phase diagrams in the $[BrO_3^-]_0$–$[I^-]_0$ plane. The plots are quite similar in shape and in the range of bistability as $[I^-]_0$ is varied. Most significant is the calculations's ability to reproduce the observed region of bistability between a stationary and an oscillatory state.

The calculated width of the bistable region as a function of $[BrO_3^-]_0$ is somewhat too large, but the main discrepancy between the two diagrams is the shift of the calculated transitions to lower $[I^-]_0$ by about 1 order of magnitude. However, it is possible to shift the critical point in the phase diagram from left to right and up and down and to narrow the region of bistability by changing k_0, the effective value of which can be modified experimentally by varying the stirring rate and/or the reactor geometry. On the other hand, it is experimentally difficult to determine the precise location of the critical point because it occurs above the limit of I_2 precipitation.

In Figure 3b, we show the calculated hysteresis in $[I_2]$ during the Hopf bifurcation as a function of k_0. Recalling that the high I_2 state corresponds to the low redox potential state, we see that the calculated and experimental behavior are qualitatively the same.

The calculated oscillatory wave forms for Br^- and I_2 are plotted in Figure 4b. They are quite similar to the ion-selective electrode and 460-nm absorbance traces of Figure 4a. In general, the model predicts somewhat smaller amplitudes and periods than observed experimentally, but detailed quantitative comparison is hampered by the dependence of these quantities and of the oscillatory flow rate range on stirring rate and reactor geometry.

Our simulations predicted that, as shown in Figure 5a, the IBr concentration should exhibit a double maximum in each cycle. After obtaining this surprising result, we measured the absorbance at 390 nm under oscillatory conditions and indeed observed two peaks per period (Figure 5b). While the IBr and Br_2 spectra do overlap significantly, comparison of the positions of the calculated $[Br^-]$, [IBr], and $[I_2]$ maxima and those of the measured ion-selective electrode potential, 390-nm and 460-nm absorbances, supports our interpretation that the 390-nm absorbance does reflect the [IBr] variation.

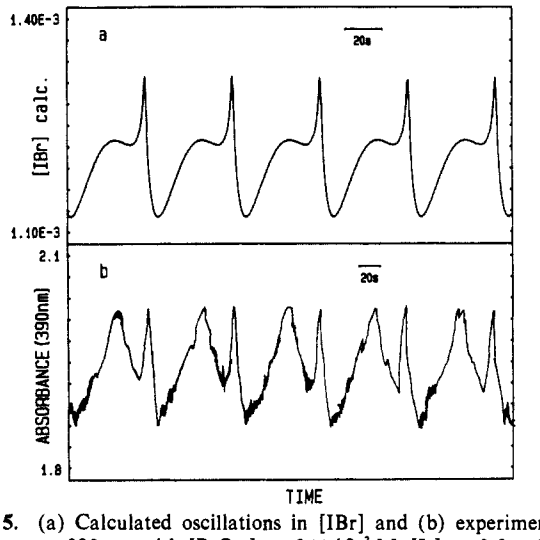

Figure 5. (a) Calculated oscillations in [IBr] and (b) experimental absorbance at 390 nm with $[BrO_3^-]_0 = 5 \times 10^{-3}$ M, $[I^-]_0 = 2.5 \times 10^{-3}$ M, $[H^+]_0 = 1.5$ M, $k_0 = 1.94 \times 10^{-2}$ s^{-1} (a), 9×10^{-3} s^{-1} (b).

Discussion

Like the mechanisms developed earlier for other chemical oscillators, the mechanism proposed here for the BrO_3^-–I^- system is complex, involving a large number of elementary steps and independent species. One may attempt to gain insight into the overall functioning of the system by examining the behavior of the species concentrations and the velocities of the elementary steps during the course of the reaction.

In Table II, we present the concentrations and rates for the two steady states under the same (bistable) conditions. In SSI, the system is well-described by three dominant steps, (E3), (E6), and (E7), which result in a net conversion of I^- and HOBr to I_2 and Br^-.

The situation in SSII is less easily characterized. The HOX and HXO_2 intermediates are present in higher concentrations, and all the rates except v_1 lie within a single order of magnitude.

Some general observations about the rates may be drawn. Reaction E1 proceeds at a negligible rate at nearly all stages of the reaction. It is of significance only in the earliest moments as a means of initiating the formation of HOI and hence I_2. In CSTR simulations, v_3 always remains within 0.1% of the value $k_0[I^-]_0$, even during transitions and oscillations. Thus, (E3) provides a nearly instantaneous conversion of the I^- flow to an I_2 input. Step E7 is a rapid equilibrium with $v_7 \sim v_{-7}$ at all times. The net difference between v_7 and v_{-7}, though small with respect to either of the individual rates, is comparable to the rates of the other elementary steps. With the exception of (E9) which may proceed in either direction, all net reaction rates lie to the right at all times.

In attempting to explain oscillatory behavior, one tends to look for autocatalytic processes. Our proposed reaction scheme is rich (perhaps too rich) in this respect. It is possible to construct a sequence of steps autocatalytic in any of several species from among reactions E1–E13. One must therefore look more closely at the behavior of the individual species during the course of the oscillation to decide which is most likely to be formed autocatalytically. On studying the concentrations (Figure 6), one is struck by the "mirror" behavior of I_2 and HOBr and by the rapid increase in HOBr as the system switches from one state to another (between points c and d in Figures 6 and 7). Examination of the rates in Figure 7 shows that the rapid formation of HOBr results from reactions E2 and E11 which combine to give the net stoichiometry of (E8). The transition from high to low I_2 begins (point a) when

$$\text{(E2)} + \text{(E11)}: \quad HBrO_2 + Br^- + H^+ = 2HOBr \qquad \text{(E8)}$$

v_2 ($\sim v_{11}$) begins to exceed v_7, which is then followed (point b) by v_6 overtaking v_3, because of the sharp increase in [HOBr].

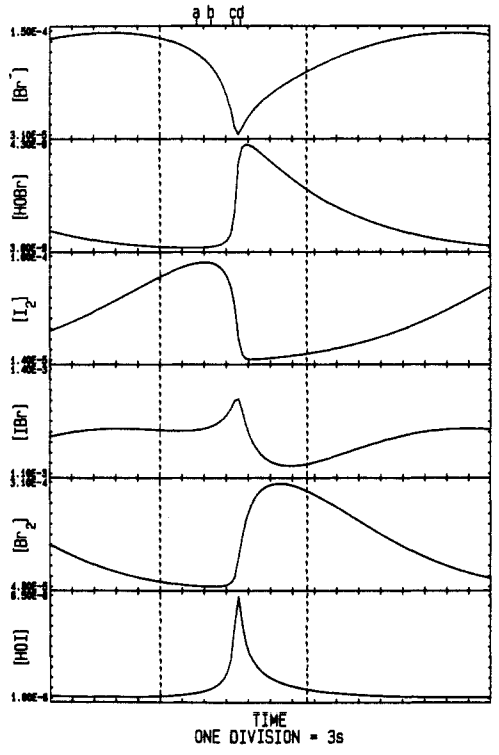

Figure 6. Calculated concentrations (M) of key species during one cycle of oscillation with $[BrO_3^-]_0 = 5 \times 10^{-3}$ M, $[I^-]_0 = 2.5 \times 10^{-3}$ M, $[H^+]_0 = 1.5$ M, $k_0 = 1.94 \times 10^{-2}$ s^{-1}.

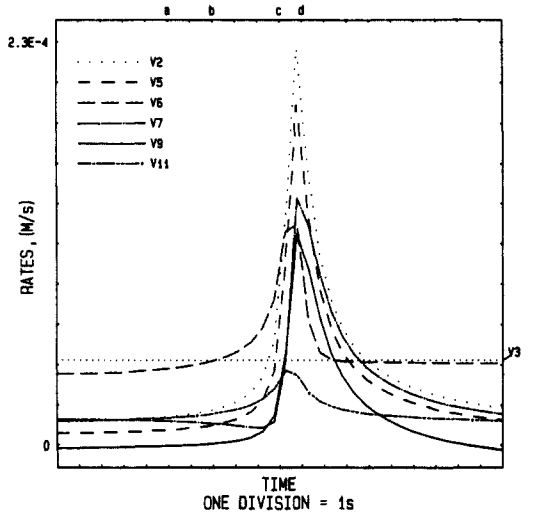

Figure 7. Calculated velocities of key reactions during the period enclosed by the dashed lines in Figure 6. For explanation of points a, b, c, and d in both figures, see text.

The sequence of overall processes during the transition, taken as the sum of the most rapid steps, is found to be

$$\text{(E2) + (E5) + (E6):}\quad I_2 + BrO_3^- \rightarrow IBr + IO_3^-$$

(point c) followed immediately by

$$\text{(E2) + (E5) + (E7) + (E9):}\quad IBr + BrO_3^- \rightarrow Br_2 + IO_3^-$$

with $v_7 > v_9$ (point d).

These observations suggest a somewhat simplified set of "key" steps:

$$\text{flow + (E3):} \xrightarrow{v_3 = k_0[I^-]_0} I_2 \qquad \text{(K1)}$$

$$\text{(E6):}\quad HOBr + I_2 \rightarrow HOI + IBr \qquad \text{(K2)}$$

$$\text{(E7):}\quad IBr + H_2O \rightarrow HOI + Br^- + H^+ \qquad \text{(K3)}$$

$$\text{(E2) + (E11) = (E8):}\quad HBrO_2 + Br^- + H^+ \rightarrow 2HOBr \qquad \text{(K4)}$$

$$\text{(E9):}\quad HOBr + Br^- + H^+ \rightarrow Br_2 + H_2O \qquad \text{(K5)}$$

The sum (K2) + (K3) + (K4) gives the autocatalytic production of HOBr accompanied by iodine consumption:

$$HOBr + I_2 + H_2O + HBrO_2 \rightarrow 2HOI + 2HOBr$$

with (E6) rate-determining. When [HOBr] becomes so large that v_6 and v_7 exceed v_2 and v_{11}, (E11) becomes rate-determining and the stoichiometry switches to

$$\text{2(K2) + 2(K3) + (K4):}\quad 2H_2O + 2I_2 + HBrO_2 + Br^- \rightarrow 4HOI + 2Br^- + H^+$$

which is now autocatalytic in Br^-. The excess HOBr and Br^- are then rapidly consumed by (K5).

When [HOBr] becomes low enough (point d–point b), $[I_2]$ increases since $v_3 > v_6$. [HOI] then builds up via hydrolysis, increasing v_2 and v_{11} until they are large enough for the HOBr autocatalysis to begin and switch the system back to the low I_2 state.

The qualitative and in some cases the quantitative agreement obtained between simulation and experiments is encouraging, particularly the reproduction of the complete phase diagram, including the region of bistability between a steady and an oscillatory state. However, our mechanism contains a large number of rate constants which have been estimated numerically. Therefore, it is possible that other sets of rate constants may give equal or better agreement. The amount of data to be modeled is considerable, and clearly experimental studies of the individual elementary steps are required before further computational effort can be justified.

The mechanism developed here resembles in certain respects the mechanisms proposed for other oxyhalogen oscillating systems. Like the $ClO_2^-I^-$ mechanism,[6] it contains no radical species but rather an interhalogen species. It also has features in common with the "bromide-controlled" bromate oscillator mechanism,[33] based on the original FKN mechanism.[2] Reaction E7, in which IBr hydrolysis acts as a source of Br^-, plays much the same role as does bromine hydrolysis in controlling oscillations in Field's recent interpretation[34] of bromate oscillations. The scheme suggested above for explaining the oscillatory behavior in the present system relies mainly on bromine- rather than iodine-containing species. Finally, we note that the present mechanism contains two, and possibly more, autocatalytic pathways as do the recent Explodator models proposed by Noszticzius et al.[35]

It should be emphasized that while our mechanism may be considered to be a hybrid of some or all of the above models, it is not reducible to any one of them. Much of the complexity in the present system may be attributed to the presence of two elements, bromine and iodine, which may be present in a variety of oxidation states and which may also combine with one another.

The success of this model in explaining the wide variety of dynamical behavior observed in the BrO_3^-–I^- reaction suggests that our mechanistic understanding of oxyhalogen oxcillators is now on a relatively sound basis. Further experimental studies of some of the proposed elementary reactions as well as computational investigations of simplified versions of the mechanism are now under way.

Acknowledgment. We thank Mohamed Alamgir, Kenneth Kustin, Robert Olsen, and Reuben Simoyi for many helpful discussions. This work was supported by National Science Foundation Grant CHE8419949.

Registry No. BrO_3^-, 15541-45-4; I^-, 20461-54-5.

(33) Noyes, R. M. *J. Am. Chem. Soc.* **1980**, *102*, 4644.
(34) Field, R. J.; Boyd, P. M. *J. Phys. Chem.* **1985**, *89*, 3707.
(35) Noszticzius, Z.; Farkas, H.; Schelly, Z. A. *J. Chem. Phys.* **1984**, *80*, 6062.